

A COVID-19 Spread Model of the Discrete Grid to Assess the Potential of Non-pharmaceutical Interventions

Wen Cao (✉ jwzx_edifier@163.com)

Zhengzhou University <https://orcid.org/0000-0003-2182-7819>

Haoran Dai

Zhengzhou University

Xiaochong Tong

Zhengzhou University

Jingwen Zhu

Zhengzhou University

Yuzhen Tian

Zhengzhou University

Feilin Peng

Zhengzhou University

Research Article

Keywords: COVID-19, Epidemiological model, Non-pharmaceutical interventions, Spatiotemporal spread model of COVID-19

Posted Date: January 18th, 2021

DOI: <https://doi.org/10.21203/rs.3.rs-143792/v1>

License: © ⓘ This work is licensed under a Creative Commons Attribution 4.0 International License.

[Read Full License](#)

1 A COVID-19 spread model of the discrete grid to assess the potential of 2 non-pharmaceutical interventions

3 Wen Cao^{1*}, Haoran Dai^{1†}, Xiaochong Tong², Jingwen Zhu¹, Yuzhen Tian¹, Feilin Peng¹

4 *Corresponding email: jwzx_edifier@163.com (Wen Cao)

5 Abstract

6 **Background:** The outbreak of COVID-19 posed a serious threat to human health, economic development, and social stability
7 worldwide, and many countries had taken different interventions to control the deterioration of the epidemic. Although many
8 studies have evaluated the effectiveness of these interventions, there were few reasonable explanations for the practical
9 geographic significance of the model parameters. Our aim was to evaluate the potential of different interventions to mitigate
10 the spread of the epidemic, including discussion about the different time and intensity of implementation, and map
11 parameters of model to the practical application meanings of the special interventions.

12 **Methods:** In this study, a COVID-19 spread model based on the discrete grid was proposed from perspective of geography. A
13 multi-level grid was introduced to describe the quarantine status and intensity in different spaces, which also combined with
14 the model of medical reception-cured and self-protection, and the spatiotemporal evolution process of early COVID-19
15 spread was simulated based on the spatial correlation, finally, the effect of interventions was quantitatively analyzed by the
16 dynamic transmission model of COVID-19.

17 **Results:** Quarantine measure were the most effective interventions, which could effectively reduce the peak value of
18 infection, advance the arrival time of the peak, and shorten the duration of the epidemic, but it only played a role under
19 sufficient intensity; the medical reception-cured and self-protection measure could effectively fatten the infection curve and
20 slowed the spread of the epidemic in the early stage, which could provide more buffer time for the relevant government
21 departments, but the practical effect was not obvious because of the limitation of actually invested resources. The role of the
22 medical reception-cured measure was more reflected in the reduction of the number of deaths, and the effect of the
23 self-protection measure could be reduced in strict quarantine measure.

24 **Conclusions:** Results of the study indicated that the quarantine, medical reception-cured and self-protection measures were
25 effective, and mitigating the spread of COVID-19 by achieving strong interventions was necessary. Strict quarantine should
26 be implementing as soon as possible in countries with serious development of COVID-19.

27 **Keywords:** COVID-19; Epidemiological model; Non-pharmaceutical interventions; Spatiotemporal spread model of
28 COVID-19;

29 1 Background

30 In late December 2019, a novel coronavirus pneumonia epidemic caused by the SARS-CoV-2 virus
31 (known as COVID-19) spread worldwide. Due to its high infection rate, long incubation period, and

32 asymptomatic infection, the virus quickly spread widely among the population, which had brought an
33 unprecedented blow to human life, economic development, and social stability ^[1-4]. In the absence of
34 effective vaccines, countries usually need to implement effective intervention measures as soon as possible
35 to alleviate the spread of COVID-19, such as strict quarantine measure, wearing face-mask, school closure,
36 and large-scale tests ^[5]. However, the unknown and sudden nature of the virus makes it difficult for people
37 to make a scientific and reasonable emergency plan policy as early as possible. Meanwhile, the large-scale
38 personnel deployment and material distribution as well as the implementation of the policy plan also need a
39 long time to prepare. Therefore, the implementation scope, implementation scale, intervention time, and
40 potential effect of the prevention and control measures are key problems to be solved urgently in all
41 countries under the condition of different degrees of COVID-19 spread, which will provide important
42 support and guarantee for scientific and effective prevention and control of infectious diseases.

43 The early researches about the COVID-19 mainly focused on epidemiology, which could be roughly
44 divided into three aspects: the estimation of the epidemiology parameters, the forecast of the epidemic
45 situation, and the analysis of the effectiveness of intervention measures. In the early stage of the outbreak
46 of COVID-19, most scholars estimated the basic reproduction number, incubation period, and other
47 epidemic parameters by using the early reported case data and overseas export data, which was helpful to
48 understand the dynamics spread mechanism of COVID-19 while preliminarily assessing the epidemic risk
49 level ^[6-10]. Subsequently, more scholars began to predict the epidemic situation, and their main idea was to
50 fit the reported case data by improving compartmental models. For example, the SEIQR、SIR-X and SIQR
51 models considering the impact of isolation measures were proposed respectively ^[11-13]; a zonal SEIRD
52 model combining the spatial diffusion and heterogeneity of infectious diseases was proposed ^[14]; the
53 SEIRS model with exponential structure was proposed ^[15]; some scholars have proposed new infectious
54 disease models by adding asymptomatic infectors and environmental infection to SEIR model ^[16-20]; some
55 stochastic based regression models were used to forecast the phenomena in as many as ten most affected
56 states of Brazil ^[21]; a hybrid ARIMA-WBF model was considered to forecast different COVID-19 infected
57 countries worldwide ^[22]; a three-stage e-ISHR introducing the time delay mechanism was established ^[23]; a
58 discrete multi-stage dynamics system with time delay based on development process of China's epidemic
59 was established ^[24]; the evolution of epidemic spread was simulated by introducing the statistical
60 characteristics of complex network distribution into epidemiological model ^[25-26]. Most of these models

61 focus on the time-series analysis of COVID-19 spread. The model parameters have a clear epidemiological
62 significance, but lacking a spatiotemporal description of practical significance. With the good effect of
63 epidemic prevention and control in some countries, many scholars began to evaluate the effect of different
64 epidemic prevention and control measures on the alleviation of epidemic situation, such as quarantine
65 [6,13,18,27-29], wearing face-mask [16,30], social distance [16,18,30-31], travel restriction [32-33], tracking and
66 isolation of cases [16,34], school closure [18], protection of the elderly over 70 years old [18], hospital isolation
67 [23,35] and external factor(ventilation and hand washing) [36-39]; some scholars evaluated the effect of
68 interventions by making statistical analysis on the trend of epidemic data in several countries^[40-42]. We
69 found that most scholars mainly aimed to estimate the effectiveness of intervention measures by adjusting
70 the model parameters to simulate the epidemic spread trend under different intervention measures based on
71 the prediction analysis model. However, there was no reasonable explanation for the mapping between the
72 model parameter values and the practical application meanings of special interventions, and few studies
73 consider that the spatiotemporal evolution of COVID-19 may have different impacts on epidemic
74 interventions. Besides, most of the models were mainly based on the compartmental model, taking the
75 epidemic area as a whole, which lacked the expression of spatial information so that it is difficult to obtain
76 the information about the spatial spread of COVID-19. Therefore, how to use the quantitative method to
77 consider spatial information and the impact of interventions in the traditional classical compartmental
78 model based on time-series process is the difficulty and focus of scientific research.

79 Geography is a discipline that studies the spatial distribution law, spatiotemporal evolution process,
80 and regional characteristics of the earth's surface geographical elements or geographical complexes, which
81 has been widely used in all walks of life. The spread and prevalence of COVID-19 is the result of a serious
82 of complex natural and social factors, and one of its most important characteristics is spatiotemporal spread,
83 which leads to understanding the phenomenon as geographical and potentially mappable^[43-44]. At present,
84 some scholars have researched in this field, such as the mobile phone data were used to forecast the
85 epidemic situation in Wuhan from the perspective of spatial interaction^[45]; the association between the
86 American nursing home-level metrics and county-level, place-based variables with COVID-19 confirmed
87 cases in nursing homes across the United States were established by using spatial modeling technology^[46];
88 the ENM was utilized to assemble the epidemic data and nine socioeconomic variables to identify the
89 potential risk zones in Beijing, Shenzhen, and Guangdong^[47]. However, the detailed and complete

90 observation data are usually difficult to obtain in a public health and safety emergency. Although these
91 studies used multi-source data to analyze the epidemic situation, it still belonged to observation and
92 reasoning under the small sample data because of the precision, resolution of data. Besides, most of the
93 current epidemic data only include the location where the patients appeared symptoms, but the location
94 where the patients were infected is rarely known, which indicates the current epidemic data also have a
95 backtracking problem. Thus how to build observation strategies and scientific methods inline the reality is
96 the key and difficult point of the current public health and safety emergencies in absence of detailed
97 observation data ^[48].

98 In this paper, we proposed a COVID-19 spread model in a discrete grid from the perspective of
99 geography. The goals of the study are two-fold; firstly, to evaluate and quantify the impacts of interventions
100 for mitigating the spread of COVID-19 by considering the spatial information, and secondly, to explain
101 reasonably the practical significance of model parameters after mapped model parameters to the practical
102 geographic area, which can provide better and more direct information to the public health and safety
103 emergencies policy. The multi-level grid was used to divide the geographical space of the epidemic area,
104 and the status and intensity of quarantine for the sub-region were described by boundary and size of the
105 grid respectively. Then the medical reception-cured model was constructed by allocating medical capacity
106 to the affected grid after considering the correlation between the spatial distribution of hospitals and the
107 grid. Besides, the proportion parameters of the self-protection population (including wearing face-mask,
108 washing hands frequently, ventilation, etc.) were introduced and mapped the corresponding grid regions to
109 achieve modeling of self-protection measure. Considering the spread way of infectious diseases usually
110 starts from the spatial adjacent to the spreading path and then gradually spreads to the surrounding region
111 (the state of free spread without human control) ^[49], the spatiotemporal spread evolution of infectious
112 diseases was simulated through the radius of people's daily life based on the spatial correlation between
113 grids when the detailed and precise population migration data (such as shared bicycle data, subway data,
114 bus data) are often difficult to obtain, and then the COVID-19 dynamics model with asymptomatic
115 infection was introduced for analyzing and quantifying epidemic spread situation in different interventions.
116 Since the epidemic prevention and control measures abroad are relatively late and loose ^[19], we used the
117 early reported cases data of the UK, US, Spain, and Germany to discuss the free spread status of
118 COVID-19 in Wuhan city under the absence of early epidemic data of Wuhan caused by sooner

119 interventions. Then the potential of quarantine measure, medical reception-cured measure, and
120 self-protection measure to alleviate epidemic spread under different scales and different intervention times
121 were discussed. Finally, the rationality and correctness of the model were evaluated with the actual
122 epidemic data, hospital distribution data, and medical attribute data in Wuhan. The novelties of this study
123 are highlighted as follows:

124 I.The association between the model parameters and the geographical space are established from the
125 perspective of geography, which makes model parameters can be mapped to the practical application
126 meanings of special interventions and provide more direct and effective information for the formulation of
127 prevention and control policies after evaluating and quantifying the potential of interventions;

128 II.According to the law that infectious diseases gradually spreads to the surrounding region starting
129 from the spatial adjacent to the infectious source, the spatiotemporal spread and evolution model of
130 COVID-19 is established in the lacking detailed observation data of crowd dynamics;

131 III.The potential effect of the medical reception-cured measure on epidemic prevention and control is
132 evaluated by allocating the capacity of medical reception and cure to the corresponding infected regions
133 from the perspective of hospital distribution.

134 **2 Methods**

135 2.1 data

136 On December 31, Wuhan reported a “viral pneumonia of unknown”, and then Wuhan issued a ban on
137 “City closure”. The government successively issued a series of measures, such as restricting transportation,
138 school closure, closing entertainment places, and prohibiting public gatherings. At the same time, many
139 designated hospitals such as “huoshenshan” and “leishenshan” as well as fangcang shelter hospitals began
140 to be put into use. Medical staff and medical resources from all over the country have been involved in the
141 fight against COVID-19 in Wuhan. In order to discuss the effect of quarantine, medical reception-cured and
142 self-protection measure to alleviate spread of infectious disease, this study collected the global epidemic
143 data including the number of confirmed cases per day, cumulative number of cured people and deaths from
144 dingxiangyuan (<https://ncov.dxy.cn/ncovh5/view/pneumonia>) and COVID-19 Data Repository by the CSSE
145 at Johns Hopkins University ^[50] (<https://www.arcgis.com/apps/opsdashboard/index.html#/bda7594740fd40299423467b48e9ecf6>); the data of designated hospitals in Wuhan, including the spatial distribution of
146 hospital, intervention times, number of open beds and cumulative number of patients from Wuhan
147

148 Municipal Health Commission, People's Daily and Baidu baike; and the data of medical resources in
149 Wuhan, including the number of local registered medical staff, the number of supporting medical staff in
150 different regions and the number of face-mask (including N95 masks and medical-surgical masks) from the
151 website of Hubei Provincial Bureau of Statistics, Hubei Provincial People's Government and People's
152 Daily.

153 When Wuhan city was closed for three weeks (February 12, 2020), the nucleic acid detection reagent
154 method was changed to clinical diagnosis (including CT method), which caused large fluctuations in the
155 cumulative confirmed cases. This problem was analyzed through Richards nonlinear curve model ^[50], and
156 according to the incubation period of COVID-19 for 7~14 days, the calibrated daily number of new
157 confirmed cases from January 29, 2020, to February 11, 2020, was shown by Table 1.

158 < **Table 1** Calibration data of newly reported cases per day in Wuhan >

159 2.2 Quarantine model based on the discrete grid

160 Quarantine measure usually takes “province - city - district - street - community - village - home” as
161 the basic unit to limit people’s activity regions, which greatly reduce the contact between the infected and
162 susceptible populations to achieve the effect of restraining the spread of infectious diseases. However, the
163 uncertainty of the size and irregular shape of the traditional prevention and control unit will bring great
164 difficulties to the modeling, and the more precise administrative division data usually is not easy to obtain.
165 According to the spatial characteristic of physical quarantine measure, the discretization of ground space
166 was realized by the multi-level global discrete grid system with different size and series grid units. An
167 adaptive statistical unit could be formed by the hierarchical geographic grid to fill the traditional prevention
168 and control unit. As shown in Fig.1, the effective grid regions were the effective areas within the
169 administrative division. The boundary and size of the grid could be used to describe the status and intensity
170 of quarantine in a region respectively, and the distribution of the grid could map the practical
171 implementation scope of quarantine measure.

172 < **Figure 1** Grid filling diagram of traditional prevention and control unit >

173 The specific design is as follows: Let the spread area of infectious diseases be A , and the research
174 areas were divided into sub-regions using the discrete grid, in which the total number of sub-regions was
175 denoted by n . Referring to the model of COVID-19 spread dynamics ^[16], the total human population in the
176 epidemic area, denoted by N , was split into susceptible humans $S(t)$, exposed humans $E(t)$, asymptomatic

177 infectious humans $A(t)$, symptomatic infectious humans $I(t)$, detected infected humans via testing $C(t)$ and
 178 recovered humans $R(t)$. The boundary of the grid was represented with a dotted line before the
 179 implementation of the quarantine measure (Fig.2). At this time, there were few restrictions on population
 180 flow, and the spread of COVID-19 was a state of free spread. The numerical changes of each population
 181 during the spread of COVID-19 could be quantified by the epidemic dynamic model of the whole region, as
 182 shown in the following equations 1~6. The related variable parameters of the model are described in Table 2.

$$183 \quad S_t = S_1 - \sum_{j=1}^{t-1} \left(\frac{\beta_0 (\alpha A_j + I_j)}{N - C_j} S_j \right) \quad (1)$$

$$184 \quad E_t = E_1 + \sum_{j=1}^{t-1} \left(\frac{\beta_0 (\alpha A_j + I_j)}{N - C_j} S_j - \sigma E_j \right) \quad (2)$$

$$185 \quad A_t = A_1 + \sum_{j=1}^{t-1} \left(\nu \sigma E_j - (\theta + \gamma_a) A_j \right) \quad (3)$$

$$186 \quad I_t = I_1 + \sum_{j=1}^{t-1} \left((1 - \nu) \sigma E_j - (\varphi + \gamma_o + d_o) I_j \right) \quad (4)$$

$$187 \quad C_t = C_1 + \sum_{j=1}^{t-1} \left(\theta A_j + \varphi I_j - (\gamma_c + d_c) C_j \right) \quad (5)$$

$$188 \quad R_t = R_1 + \sum_{j=1}^{t-1} \left(\gamma_c C_j + \gamma_a A_j + \gamma_o I_j \right) \quad (6)$$

189 When the quarantine measure was implemented, all grid boundaries changed from the dotted line to
 190 solid lines, and the current time was denoted by t_0 . The activities of the population would be limited in the
 191 sub-regions so that COVID-19 could only spread in the grid regions and couldn't affect the other grid
 192 regions (Fig.2). The number of different humans in the sub-grid was denoted by S_i^t , E_i^t , A_i^t , I_i^t , C_i^t and
 193 R_i^t at time t respectively, and the numerical changes of each human were the sum of all sub-regions, as
 194 shown in the following equation 7~12, where N_i was the number of population in each grid, and its
 195 specific value was obtained from the statistical yearbook data using Kriging interpolation ^[49].

$$196 \quad S_t = \sum_{i=1}^n \left(S_i^{t_0} - \sum_{j=1}^{t-1} \frac{\beta_0 (\alpha A_i^j + I_i^j)}{N_i - C_i^j} S_i^j \right) \quad (7)$$

$$197 \quad E_t = \sum_{i=1}^n \left(E_i^{t_0} + \sum_{j=1}^{t-1} \left(\frac{\beta_0 (\alpha A_i^j + I_i^j)}{N - C_i^j} S_i^j - \sigma E_i^j \right) \right) \quad (8)$$

$$198 \quad A_t = \sum_{i=1}^n \left(A_i^{t_0} + \sum_{j=1}^{t-1} \left(\nu \sigma E_i^j - (\theta + \gamma_a) A_i^j \right) \right) \quad (9)$$

$$199 \quad I_t = \sum_{i=1}^n \left(I_i^{t_0} + \sum_{j=1}^{t-1} \left((1 - \nu) \sigma E_i^j - (\varphi + \gamma_o + d_o) I_i^j \right) \right) \quad (10)$$

$$200 \quad C_t = \sum_{i=1}^n \left(C_i^{t_0} + \sum_{j=1}^{t-1} \left(\theta A_i^j + \varphi I_i^j - (\gamma_c + d_c) C_i^j \right) \right) \quad (11)$$

$$201 \quad R_t = \sum_{i=1}^n \left(R_i^{t_0} + \sum_{j=1}^{t-1} \left(\gamma_c C_j + \gamma_a A_j + \gamma_o I_j \right) \right) \quad (12)$$

202 < **Figure 2** Schematic diagram of the quarantine measure model based on a discrete grid >

203 < **Table 2** Parameters description of COVID-19 spread dynamics model >

204 2.3 Spatiotemporal spread model of COVID-19 based on the discrete grid

205 The most important character of infectious diseases is that their spread needs certain ways of spread,
 206 such as air spread, droplet spread, close contact, and blood spread. Government departments usually take
 207 prevention and control measures to reduce the frequency of contact between infected humans and
 208 susceptible humans, such as strict quarantine, testing, and tracking of cases, wearing face-mask, and
 209 actively keeping distance with fever patients. Thus we need to mater more information about the spread of
 210 infectious diseases to evaluate the effect of prevention and control measures, that is, the distribution of the
 211 number of infectious humans in each grid at different times.

212 The differences of regions and virus type make the spatiotemporal spread mode, spread path, and
 213 spread capacity of infectious diseases have certain differences, but, in general, the spread of infectious
 214 diseases usually gradually spreads to the surrounding regions starting from the place adjacent to the spread
 215 path space ^[49]. The number of newly infected people in a sub-region at a certain time is not only affected by
 216 the number of infectious people in the previous time but also affected by the number of infectious people in
 217 the surrounding regions in the previous time when the population flow in the epidemic area is not
 218 completely limited, in other words, the infected grid includes the status of self-infection and mutual
 219 infection (Fig.3). Thus the epidemic area was intersected with the buffer of infected grids constructed by
 220 the people's average living radius to get the daily new infected grid regions, which denoted by r , and the

221 incompletely infected grid was regarded as infected for the convenience of calculation.

222 In the process of the spread of infectious diseases, the number of newly infected cases per day always
223 has a time-series change process that increases first and then decreases, and the infected people are
224 composed of many discrete points in space. According to Tobler's first law of geography, the spread of
225 infectious diseases restricted by geographical spatial factors has a strong spatial correlation characteristic
226 [44]. The distance was used to describe the spatial weight concept of the infected grids, which could allocate
227 the number of newly infected people at the next moment to the corresponding infected grid, as shown in
228 Fig.3 and equations 13~14.

$$229 \quad W_i^t = \left(h_{ij}^t \right)^{-p} / \sum_{i=1}^{n^t} \left(h_{ij}^t \right)^{-p} \quad (13)$$

$$230 \quad h_{ij}^t = \sqrt{\left(x_i^t - x_j^{t-1} \right)^2 + \left(y_i^t - y_j^{t-1} \right)^2} \quad (14)$$

231 where W_i^t is the weight for the number of newly infected people assigned by the infected grid, h_{ij}^t is the
232 distance from the infected grid to the affected grid, $\left(x_i^{t-1}, y_i^{t-1} \right)$ is the coordinates of the center point of the
233 infected grid, $\left(x_j^{t-1}, y_j^{t-1} \right)$ is the coordinates of the center point of the affected grid, and n^t is the number
234 of the affected grid, and p is any positive real number, usually 2.

235 < **Figure 3** Spatiotemporal spread model for infectious diseases based on a discrete grid >

236 2.4 The model of Self-protection measure

237 During the outbreak of COVID-19, some common self-protection measures of the susceptible
238 humans and infected humans can reduce the spread rate of COVID-19, such as wearing face-mask
239 effectively, washing hands frequently, keeping ventilation in the house, and keeping distance with fever
240 patients actively. Clinical and infectious disease studies have shown that proper self-protection measures
241 could effectively reduce the risk of infection and the external spread of the virus by 70%~80% [52]. In this
242 study, a parameter ε was introduced to represent the population proportion of effective self-protection in the
243 total population and could be mapped to each grid region. The infected probability of susceptible humans
244 with the effective self-protection was reduced to 30% of the normal value, while the infected rate and
245 external spread rate of other people remained unchanged (Fig.4A).

246

247 2.5 The model of medical reception-cured measure

248 During the spread of COVID-19, the government opened designated hospitals and set up outpatient
 249 clinics to detect and receive suspected patients. People usually took the nearby hospital to diagnosis when
 250 they found themselves uncomfortable under the influence of people's living, work, activity range, and the
 251 surrounding environment. Therefore, the spatial distribution of hospitals and the number of beds has a great
 252 impact on the spread of infectious diseases, and there is a strong spatial correlation between the
 253 geographical space and hospital. Considering the open time lag of medical beds and government
 254 investment in medical beds is usually based on the number of currently infected people, the percentage
 255 parameter δ for the number of infected people was introduced to simulate the number of beds put into
 256 use in the hospital every day, and then the number of cases admitted to hospital every day will be allocated
 257 to the corresponding infected grid based to the spatial distance weight (Fig.4B), where Q_A and Q_I are
 258 the number of asymptomatic and symptomatic infected people admitted in the hospital every day
 259 respectively, and specific values are assigned to $\sum_{i=1}^n Q_i^t$ according on the corresponding detection ratio (θ
 260 and φ). The number of daily medical reception-cured patients in each grid is shown in the following
 261 equations 15~17.

$$262 \quad h_{ij} = \sqrt{(x_i - x_j)^2 + (y_i - y_j)^2} \quad (15)$$

$$263 \quad W_{ij} = h_{ij}^{-p} / \sum_{j=1}^{n_i} h_{ij}^{-p} \quad (16)$$

$$264 \quad Q_i^t = \begin{cases} 0, t \leq t_j^0 \cup t \geq t_j^1 \\ \sum_{j=1}^H w_{ij} \times \delta \times (A_t + I_t), t_j^0 \leq t \leq t_j^1 \end{cases} \quad (17)$$

265 where Q_i^t is the number of patients admitted by the hospital in the grid (asymptomatic and symptomatic),
 266 h_{ij} is the distance between the grid and the hospital, w_{ij} is the assigned weight of the number of hospital
 267 patients in the corresponding grid, (x_i, y_i) is the coordinates of the central point of the infected grid,
 268 (x_j, y_j) is the coordinates of hospital, n_i is the number of the grid affected by the hospital, and t_j^0 t_j^1
 269 are the intervention time and closing time of the hospital respectively.

270 < **Figure 4** Schematic diagram of medical reception-cured measure (A) and self-protection measure (B) >

271 **3 Results**

272 3.1 Numerical simulation and analysis for the original spread state of COVID-19

273 In this section, the possible trend of the epidemic without any interventions in Wuhan was discussed to
274 prepare the subsequent assessment for the impacts of intervention measures to mitigate the spread of the
275 COVID-19 epidemic. The first thing to be clear is that no country will allow infectious diseases to spread
276 freely, which means that the original spread state of any infectious diseases is usually not available. At
277 present, many scholars used the early epidemic data of the study area or random sampling of the basic
278 reproduction number R_0 to solve this issue [16,18]. Unfortunately, Wuhan is the first city in the world to
279 openly face the COVID-19 epidemic. Due to the unknown characteristic of the virus and the rapid and
280 intensive intervention measures, the number of early data samples in Wuhan are too few and cannot truly
281 describe the early spread trend of the COVID-19. However, interventions in foreign regions are relatively
282 late and loose [19], which makes it is more likely that their early epidemic data is consistent with the real
283 spread situation of COVID-19. But, the differences in the extent of COVID-19 spread, patterns of
284 population movement, and levels of economic development in different regions make it difficult to state
285 objectively and accurately which country's data are most appropriate for simulating the spread trend of
286 COVID-19. Therefore, these studies selected the early epidemic data of the UK, the US, Spain, and
287 Germany to discuss the original spread situation of COVID-19.

288 Our simulation is based on the genetic algorithm to estimate the parameters by regarding the daily
289 number of confirmed patients as the adaptive index, and the other parameter values of the COVID-19
290 spread dynamic model are shown in Table 3. Clinically, the average incubation period of COVID-19 is 5.2
291 days, ranging from 3 to 14 days. We assumed that the data within 14 days after the strict measures are still
292 early data, which was to avoid the phenomenon that the early sample data was too small to be estimated
293 accurately. It is worth noting that our estimation started from the announcement of the first confirmed case in
294 each country, but there were already unknown numbers of infected and exposed humans in the population
295 at that time. Therefore, the estimation parameters included the estimation of the first day exposed cases E_1 ,
296 asymptomatic cases A_1 and symptomatic cases I_1 . We repeated the genetic algorithm 100 times to ensure the
297 reliability of the results. The results are shown in Fig.5, and the corresponding estimated parameter values
298 are shown in Table 4. Here, the time of early epidemic data in the UK, the US, Spain, and Germany is from
299 January 31, 2020 to April 3, 2020, January 20, 2020 to March 28, 2020, February 1, 2020 to March 28,

2020, and January 27, 2020, to March 24, 2020, respectively.

< **Table 3** Values of parameters in the COVID-19 spread dynamics model epidemic model >

< **Figure 5** The number of newly reported cases per day of original state simulated by genetic algorithm (Small chart section: the red histogram represents the early epidemic data of each country, and the curve is the original spread state curve of COVID-19 in each country. Here, the starting time of X coordinate in the UK, the US, Spain, and Germany is January 31, 2020, January 20, 2020, February 1, 2020, and January 27, 2020, respectively; big graph section: the solid-line curve is the original spread state curve of Wuhan. The red dotted-line curve shows the actual number of newly reported cases in Wuhan after calibration, and the purple dotted-line curve represents the actual number of newly reported cases in Wuhan. Here, the starting time of X coordinate in the Wuhan is December 28, 2020^[9] >

<**Table 4** Parameters of the COVID-19 original spread state curve estimated by genetic algorithm>

Fig.5 shows that: the results of the model to fit the early data of each country were better (small chart section in Fig.5). After bringing the fitting parameters to the COVID-19 dynamic model of Wuhan, the original spread state of COVID-19 compared to the real curve in Wuhan was mainly reflected in the improvement of peak value, the extension of peak arrival time, and the continuous-time of epidemic situation. However, although the early data was fit well (the small part in Fig.4), the future trend of each curve was quite different, mainly in the number of peaks. This difference was because the spread of the early epidemic was easily affected by the population distribution, population flow, and the efficiency of medical resource detection in different regions. Alberti et al. also pointed out that there was great uncertainty in using early data to predict the epidemic situation, and there is a big scientific verification problem in forecasting with small sample data^[53].

Table 4 shows that infection rate β_0 , asymptomatic detection rate θ , symptomatic detection rate φ , and basic reproduction number R_0 in the estimated parameters were roughly the same (the same countries), among the estimation of R_0 was similar to Wu^[6], Zhou^[7] and Wang^[9]. However, the estimated values of E_1 , A_1 and I_1 were quite different, mainly because it was difficult to confirm the actual number of infected people who had already exited but had not been tested or had no symptoms in the population when the first case was found.

In sum, we selected 10 different original spread parameters estimated by the early data of the UK, the

328 US, Spain, and Germany for the COVID-19 dynamic spread model of Wuhan to make up for the difficulty
329 of obtaining the original spread state of COVID-19 in Wuhan, and then try to estimate the effect of
330 different interventions to mitigate the spread of the COVID-19, which eliminated the difference for
331 potential assessment of prevention and control measures under different COVID-19 original spread.

332 3.2 Experimental analysis for the influence of different quarantine measure to mitigate the spread of 333 COVID-19

334 This part mainly discussed the influence of quarantine measure with different intensities and
335 intervention times to mitigate the spread of the COVID-19. The grid size represented the strength of the
336 quarantine measure, that is, the corresponding quarantine measure became more stringent with grid size
337 became finer. We took the intervention time when Wuhan city issued a ban on “city closure” as the baseline,
338 and set the grid size to 1000 m, 500 m, 250 m, 100 m, and 10 m respectively (Fig.6A). Then, we fixed the
339 grid size of 10 m and adjusted the intervention time into 41st day, 44th day, 47th day, 50th day, and 53rd
340 day respectively (Fig.6B). The average daily life radius of people was 2000 m, which was based on the
341 travel characteristics of Wuhan residents ^[54].

342 < **Figure 6** The change curve of newly reported cases per day in Wuhan under different quarantine measure >

343 Fig.6A shows that: whatever the scale of the original spread curve of COVID-19, the curves would be
344 close to the actual epidemic curve of Wuhan with the decrease of grid size, which was mainly reflected in
345 the reduction of peak infection, the shortening of peak arrival time and epidemic duration. No matter what
346 kind of original infection state, the original spread curves of COVID-19 was almost not changed at 500 m
347 grid. This mainly because the spread of infectious diseases are easily affected by population flow and
348 population distribution, but the 500 m grid does not limit the contact of the population, which shows that
349 quarantine measure must reach a certain intensity to be effective, especially the home quarantine state (10 m
350 grid). From the perspective of the severity of different original spread state, the peak infection, the time of
351 peak arrival, and the duration of the epidemic situation were greatly reduced for the curve with a very
352 serious spread degree. However, although the curve with a relatively light original spread state would
353 decrease with the increase of grid size, it seems that the scale of reduction was much smaller. Thus we
354 suggest that quarantine measure is a very effective epidemic prevention and control measure, especially for
355 viruses with high infectious characteristics, and it also seems to be not necessary to use when the epidemic
356 situation is relatively light because strict quarantine measure needs to invest unimaginable financial,

357 material and human resources. This seems to have been demonstrated in South Korea and Japan^[5]. From the
358 perspective of the final results of the 10 m grid, even if the original spread trend of all curves were different,
359 the final curves almost coincided. This is mainly because the role of quarantine measure is to protect the
360 uninfected population by limiting the activities of the population. When the grid is very small, there are few
361 people that infectious people can contact so that most of the uninfected people are protected, which makes
362 the number of final infected people is almost the same.

363 Fig.6B shows that: the epidemic curve deviated from the actual curve in Wuhan with the delay of
364 intervention time, which mainly reflected in the increase of peak value, the extension of peak arrival time,
365 and epidemic duration. Compared with the actual epidemic curve in Wuhan, the number of new confirmed
366 cases per day had more than doubled just one week later, which also emphasizes that quarantine measure
367 need timely intervention to achieve better results.

368 3.3 Experiment analysis for the influence of different self-protection measure to mitigate the spread of 369 COVID-19

370 This part mainly discussed the influence of self-protection measure with different proportions of
371 effective self-protection population and quarantine intensities to mitigate the spread of the COVID-19. We
372 took the intervention time when a group of pneumonia cases with unknown etiology were first published in
373 Wuhan municipal health commission (January 11, 2020) as the baseline, and set the proportion of
374 self-protection population to 0.1, 0.2, 0.3, and 0.4 of the total human respectively (Fig.7A). Then, we
375 adjusted the proportion of self-protection personnel to 0.1, 0.2, 0.3, and 0.4 under the grid size of 500 m,
376 250 m, 100 m, and 10 m, respectively (Fig.7B).

377 < **Figure 7** The change curve of newly reported cases per day in Wuhan under different self-protection measure >

378 Fig.7A shows that: the original spread curve of COVID-19 gradually moves away from the actual
379 curve of Wuhan with increasing the proportion of the self-protection population. However, it seemed that
380 only the duration of the epidemic and the time to reach the peak would only increase, but the peak of
381 infection was gradually declining. This is mainly because self-protection measure does not fundamentally
382 cut off the spread of the virus, and only reduce the infected probability. The total population of Wuhan is
383 about 14 million. Even if it is based on the ratio of 0.1, the number of people who need to achieve effective
384 self-protection every day in Wuhan will reach 1.4 million. In terms of the number of face-mask, this is an
385 unimaginable expense. Therefore, we suggest that the role of self-protection measure mainly is to delay the

386 arrival of epidemic peak and strive for more preparation time for the government.

387 Fig.7B shows that: under the grid of 500 m and 250 m, the peak value of the COVID-19 spread curve
388 decreased and the time to reach the peak value was delayed with the increase of the proportion of effective
389 self-protection population. However, the COVID-19 spread curve hardly changed under the grid of 100 m
390 and 10 m. This is mainly because the strict quarantine measure makes the movable area of infectious
391 patients very small, and self-protection measure is difficult to achieve an effect at this time, which also
392 shows that some resources of self-protection measure, such as face-masks, medical clothes, hand sanitizer,
393 and disinfectant, can be concentrated in the hands of high-risk groups who have to go out or need to contact
394 with infected patients, such as medical staff, material distribution staff and relevant leaders under strict
395 quarantine measure.

396 3.4 Experiment analysis for the influence of different medical reception-cured measure to mitigate the
397 spread of COVID-19

398 This part mainly discussed the influence of medical reception-cured measure with different medical
399 beds and intervention time to mitigate the spread of the COVID-19, and the number of medical beds was
400 calculated according to the percentage of daily existed infected people (including symptomatic cases and
401 asymptomatic cases). We took the intervention time when the first batch of designated hospitals in Wuhan
402 (January 20, 2020), and set the proportion of medical beds to 0.1, 0.2, 0.3, and 0.4 respectively (Fig.8A &
403 Fig.8B). Then, we fixed the ratio of bed investment was 0.1 and adjusted the intervention time into 34th day,
404 37th day, 40th day, 43rd day, and 46th day, respectively (Fig.8C).

405 < **Figure 8** The change curve of newly reported cases per day in Wuhan under the different medical
406 reception-cured measure (the length of the yellow vertical line and the green prism points indicates the 95%
407 confidence interval and the median values of the total number of invested beds corresponding to 10 curves
408 in group B, respectively) >

409 Fig.8A shows that: the original spread curve of the COVID-19 decreased at the peak with the increase
410 of beds (the proportion increased), which emphasized the effectiveness of the medical reception-cured
411 measure. However, the time of peak arrival and the duration of the epidemic did not seem to change. This is
412 mainly because there are a large number of undetected or ineffectively quarantined cases in the population
413 when the medical reception-cured measure is put into use. Thus the medical bed will soon reach full load
414 because of the limitation of the medical beds. Fig.8B shows the total number of medical beds required to be

415 invested was about 580000 at the proportion of 0.1, which is difficult to meet in reality.

416 Fig.8C shows that: the original spread curve shifted to the left with the intervention time moved
417 forward, which was mainly reflected in the increase of peak arrival time and epidemic duration, but the
418 peak did not seem to change. After maintaining a low level of epidemic spread for short time, the medical
419 beds would reach the load, and the epidemic would break out again on a large scale. At this time, the
420 medical system has collapsed and the scale of the outbreak again was similar to the original spread state,
421 and the US seems to be facing the same problem. Therefore, we suggest that other effective measures must
422 adopt to reduce the pressure on the medical system.

423 3.5 Model validation under actual interventions of COVID-19 in Wuhan

424 In this part, the actual quarantine intensity, the number of medical beds, and the proportion of effective
425 wearing face-mask (self-protection measure) were used to verify the reliability of the model. In terms of
426 quarantine measure, we used the 10 m grid to approximately represent the home quarantine measure
427 implemented in Wuhan, and the intervention time was January 24, 2020, when Wuhan issued a ban on
428 “lockdown”. For the medical reception-cured measure, there were 68 designated hospitals in Wuhan,
429 including 16 fangcang shelter hospitals, "huoshenshan" and "leishenshan" hospitals, with a total of 38782
430 beds. Thus our proportion of beds was approximately 0.06 of the daily existed infected people in the
431 different original spread curves (including symptomatic and asymptomatic), and the intervention time was
432 the time when the first batch of designated hospitals began to put into operation (January 20, 2020). Due to
433 the number of humans complying with the self-protection measure was difficult to obtain, the proportion of
434 self-protection measure in Wuhan was represented by the proportion of effectively wearing face-mask. We
435 assumed each medical staff used two face-masks every day and every citizen consumed one face-mask
436 every three days. Thus Wuhan needs to consume 2.1744 million face-masks per day referring to the total
437 number of medical staff in Wuhan was about 108 720 (including local medical staff and support medical
438 staff) and the total population of Wuhan was about 14.18 million. According to the statistics, Wuhan
439 received a total of 55.1 million face-masks (including N95 masks and medical-surgical masks) during the
440 period from February 3, 2020, to February 13, 2020. Therefore, we set the daily effective proportion of
441 wearing masks was 0.1 and the intervention time of self-protection measure was the time when a group of
442 pneumonia cases with unknown etiology were first published in Wuhan municipal health commission
443 (January 11, 2020). The results are shown in Fig.9.

444 < **Figure 9** The change curve of newly reported cases per day in Wuhan under actual interventions >

445 Fig.9 shows that: the original propagation curve continuously shrunk to the actual epidemic curve of
446 Wuhan and the final result was almost consistent with the actual curve of Wuhan under the three
447 interventions, which also showed the effectiveness of the model in this study. Among them, quarantine
448 measure was the most effective, and medical reception-cured measure and self-protection measure were
449 mainly reflected in reducing the peak of infection and delaying the spread of the COVID-19 in the early
450 stage (the curve moved to the left). However, there is some deviation between the final curve and the actual
451 curve of Wuhan, which is mainly because of the following reasons: 1) it has a certain difference that the
452 original spread trend of the COVID-19 estimated by the early data of other countries brought into Wuhan
453 city itself; 2) there will be some errors in the case detection and data recording in Wuhan city because of
454 the large amount of unknown information about the new virus in the early stage; 3) there is still an obvious
455 difference between the distribution of population and the actual situation, such as there is no crowd activity
456 for the lakes, fields, and wasteland.

457 **4 Discussion**

458 Facing the increasingly serious threat of COVID-19, all countries urgently need to use computer
459 modeling to determine the best strategy to mitigate the impact of COVID-19 [5]. The type of intervention
460 measures, the intensity of implementation, the scope of implementation, and the intervention time are
461 different in different countries because of the differences of the geographical environment factors such as
462 the evolution state of the epidemic, urban building distribution, human's lifestyle, and economic
463 development, etc. However, this is also the key to the effectiveness of COVID-19 prevention and control.
464 We aim to put forward a model that can integrate spatial and temporal information to further consider the
465 development law of COVID-19 under the influence of more complex natural and social factors, to master
466 more deep information about the spatiotemporal spread pattern of the COVID-19 and epidemic prevention
467 and control. Meanwhile, it also can explain the practical significance of the model parameters by mapping
468 the model parameters to the geographical space, which can provide more direct instructive information for
469 the implementation of specific invention policies after scientifically and reasonably evaluating and quantifying
470 the potential of interventions. But this study has several notable limitations:

471 Due to the existing data on epidemic cases were not complete, we believed that there were still many
472 uncertainties in the research on the mechanism of COVID-19 dynamic spread, such as the proportion of

473 asymptomatic infected people and the asymptomatic spread rate. Although the model parameters of this
474 study referred to the research of articles in famous international journals [1,16,54], a large number of unknown
475 parameters were ineluctably included in the quantitative model of COVID-19. However, it was worth
476 noting that our focus was not on the forecast of the epidemic situation in various regions, and the curve
477 parameters of the COVID-19 dynamics model were mainly used to evaluate and quantify the impact of
478 interventions. The relevant conclusions were consistent with recent studies [5,13,16,23]. Besides, due to the
479 lack of spatiotemporal attribute data such as population data, traffic data, building data, and human
480 migration data, we had not established the relationship between the grid and corresponding geographic
481 attributes. Therefore, the population distribution and COVID-19 spread model in this study was a kind of
482 approximate simulation of the actual situation combining with the objective law from the perspective of the
483 whole, which aimed to prepare for the subsequent evaluation of the potential of interventions. Meanwhile,
484 the author indicates that even if the detailed epidemic data can be obtained, it only includes the location
485 where patients showed symptoms, but the location of the infection is still not known, in other words, the
486 current spread models of the COVID-19 have the problem of scientific. Nevertheless, our results for the
487 spread of the COVID-19 were consistent with a recent work in which predicted the epidemic situation in
488 different regions based on the SEIRD model [55].

489 This study preliminarily revealed objectively the spatiotemporal spread distribution law and
490 development trend of COVID-19 from the perspective of geography and established the relationship
491 between the model parameters and the actual geographical significance. We intended to use the available
492 data to simulate the more complex phenomenon of the spread of COVID-19 in reality, such as data of urban
493 travel and crowd migration data, to enhance the authenticity of the model although complete observation
494 data was difficult to obtain. In future work, we hope to solve the problem of scientific verification of
495 interventions model through multi-source data, such as network news data, global event database, and
496 remote sensing data. The model also considered the impact of hospitals' spatial distribution on the
497 prevention and control of the COVID-19, which also provided a possible way to analyze the problem about
498 the medical resource allocation, spatial location selection, and overall planning of medical admission in
499 different regions. Finally, the mapping between social-economic data and grid areas can be established to
500 quantify the cost of economy and resources under different interventions, which provides more guidance
501 for scientific decision-making and accurate implementation for prevention and control of COVID-19. To

502 sum up, these will be the focus and difficulty of our subsequent research.

503 **5 Conclusion**

504 In summary, this study combined the COVID-19 dynamic spread model with geography from a new
505 perspective to quantitatively analyze the impacts of prevention and control measures. The discrete grid was
506 used to divide the geographical regions and the spatiotemporal spread model of COVID-19 was designed
507 based on the correlation between infected cases, hospital, and the grid. Meanwhile, the model parameters of
508 interventions were mapped to the corresponding grid regions, and finally, the COVID-19 dynamic model
509 was used for quantitative analysis. Through the simulation of the original spread status of COVID-19 and
510 the actual epidemic data in Wuhan, the conclusions are as follows:

511 1) Quarantine measure was the most effective measure for epidemic prevention and control. The main
512 role of the quarantine measure was to reduce the number of infection peaks, advance the arrival time of the
513 peak, and shorten the duration of the epidemic, especially for infectious diseases with high infectivity.
514 However, the quarantine measure must be effective under sufficient intensity, and the effect of the
515 quarantine measure would become lower with the delay of intervention time. Besides, strict quarantine
516 measure may be avoided in the early stages of the outbreak which the spread of the epidemic is mild.

517 2) Medical reception-cured measure played mainly a part in the early stage of the COVID-19 outbreak.
518 The increase of medical beds could significantly reduce the peak of the epidemic but had little effect on the
519 arrival time of peak and duration of the epidemic. Besides, the early intervention time could significantly
520 delay the arrival of the infection peak. However, the outbreak would still occur again and the scale was
521 similar to the original infectious state when the medical beds reached full load.

522 3) Self-protection measures could reduce the number of peak and delay the arrival time of the peak and
523 duration of the epidemic, which could give the government more buffer time. However, the self-protection
524 measure almost had no effects under the strict quarantine measure. Besides, the medical resources could be
525 concentrated in hospitals and other places in urgent need under strict quarantine measure.

526 4) The model in this study could analyze qualitatively and quantitatively the impacts of quarantine
527 measure, self-protection measure, and medical reception-cured measure to slow the spread of epidemic
528 considering spatial information of the COVID-19, which was scientific and reasonable. Meanwhile, it had
529 high interpretability for the practical significance for intervention model parameters and could map the
530 model to the actual geographical area, which is helpful for the scientific formulation of specific epidemic

531 prevention and control decision.

532 **Abbreviations**

533 COVID-19: Coronavirus disease 2019; SEIQR: susceptible - exposed - infected - quarantined -
534 recovered; SIR-X: susceptible-infectious-X; SIQR: Susceptible - Infectious - Quarantined - Recovered;
535 SEIRD: susceptible - exposed - infected - recovered - deceased; SEIRS: susceptible - exposed - infectious -
536 recovered - susceptible; e-ISHR: exposed - infected - susceptible - hospital - recovered; ENM: ecological
537 niche models; CT: Computed tomography; CSSE: Center for Systems Science and Engineering.

538 **Acknowledgments**

539 None.

540 **Authors' contributions**

541 Wen Cao and Haoran Dai in Conceptualization, methodology, Writing - original draft, Writing -
542 review & editing. Xiaochong Tong in Funding acquisition. Jingwen Zhu, Yuzhen Tian and Feilin Peng in
543 providing critical feedback and edits to subsequent revisions.

544 **Funding**

545 This study was funded by the National Key Research and Development Program of China
546 (2018YFB0505304) and the National Natural Science Foundation of China (Grant No. 41671409).

547 **Availability of data and materials**

548 Not applicable.

549 **Ethics approval and consent to participate**

550 Not applicable.

551 **Consent for publication**

552 Not applicable.

553 **Competing interests**

554 The authors declare no conflicts.

555 **Authors details**

556 ¹ School of Geoscience and Technology, Zhengzhou University, Zhengzhou, China

557 ² School of Geospatial Information, University of Information Engineering, Zhengzhou, China

558 [†]These authors contributed equally to this article and share first authorship.

559 **References**

- 560 [1] Chen N, Zhou M, Dong X, et al. Epidemiological and clinical characteristics of 99 cases of 2019 novel coronavirus pneumonia in
561 Wuhan, China: a descriptive study. *The Lancet*. 2020; 395 (10223): 507-513. [https://doi.org/10.1016/S0140-6736\(20\)30211-7](https://doi.org/10.1016/S0140-6736(20)30211-7).
- 562 [2] Li Q, Guan XH, Wang XY, Wu P, et al. Early spread dynamics in Wuhan, China, of novel coronavirus-infected pneumonia.
563 *National England Journal Medicine*. 2020; 382: 1199-1207. <https://doi.org/10.1056/NEJMoa2001316>.
- 564 [3] Tian HY, Liu YH, Li YD, et al. An investigation of spread control measures during the first 50 days of the COVID-19 epidemic in
565 China. *Science*. 2020; 6491(368): 638-642. <https://doi.org/10.1126/science.abb6105>.
- 566 [4] Chan J, Yuan SF, Kok K, et al. A family cluster of pneumonia associated with the 2019 novel coronavirus indicating person - to -
567 person spread: a study of a family cluster. *The lancet*. 2020; 395 (10223): 514-523. [https://doi.org/10.1016/S0140-6736\(20\)30154-9](https://doi.org/10.1016/S0140-6736(20)30154-9).
- 568 [5] Currie CSM., Fowler JW, Kotiadis K, et al. How simulation modeling can help reduce the impact of COVID-19. *Journal of*
569 *simulation*. 2020; 2(14): 83-97. <https://doi.org/10.1080/17477778.2020.1751570>.
- 570 [6] Wu JT, Leung K., Leung GM. Nowcasting and forecasting the potential domestic and international spread of the 2019-nCoV
571 outbreak originating in Wuhan, China: a modelling study. *The Lancet*. 2020; 10225(395): 689-697.
572 [https://doi.org/10.1016/S0140-6736\(20\)30260-9](https://doi.org/10.1016/S0140-6736(20)30260-9).
- 573 [7] Wang HW, Wang ZZ, Dong YQ, et al. Phase-adjusted estimation of the number of Coronavirus Diseases 2019 cases in Wuhan,
574 China. *Cell Discovery*. 2020; 6: 10. <https://doi.org/10.1038/s41421-020-0148-0>.
- 575 [8] Zhao S, Lin QY, Ran JJ, et al. Preliminary estimation of the basic reproduction number of novel coronavirus (2019-nCoV) in China,
576 from 2019 to 2020: A data-driven analysis in the early phase of the outbreak. *International Journal of Infectious Diseases*. 2020; 92:
577 214-217. <https://doi.org/10.1016/j.ijid.2020.01.050>.
- 578 [9] Zhou T, Liu Q, Yang Z, et al. Preliminary prediction of the basic reproduction number of the Wuhan novel coronavirus 2019-nCoV.
579 *Journal Evidence-Based Medicine*. 2020; 13: 3-7. <https://doi.org/10.1111/jebm.12376>.
- 580 [10] Read J.M, Bridgen JRE, Cummings DAT, et al. Novel coronavirus 2019-nCoV: early estimation of epidemiological parameters
581 and epidemic predictions. *medRxiv* 2020.01.23.20018549. <https://doi.org/10.1101/2020.01.23.20018549>.
- 582 [11] Jumpen W, Wiwatanapataphee B, Wu YH, et al. A SEIQR model for pandemic influenza and its parameter identification.
583 *International Journal of Pure and Applied Mathematics*. 2020; 52(2): 247-265. <http://ijpam.eu/contents/2009-52-2/8/index.html>.
- 584 [12] Maier BF, Brockmann D. Effective containment explains sub-exponential growth in confirmed cases of recent COVID-19
585 outbreak in Mainland China. *Science*. 2020; 368(6492): 742-746. <https://doi.org/10.1126/science.abb4557>.
- 586 [13] Crokidakis N. COVID-19 spreading in Rio de Janeiro, Brazil: Do the policies of social isolate-on really work?. *Chaos, Solitons &*
587 *Fractals*. 2020; 136: 109930. <https://doi.org/10.1016/j.chaos.2020.109930>.
- 588 [14] Viguerie A, Lorenzo G, Auricchio F, et al. Simulating the spread of COVID-19 via a spatially-resolved susceptible - exposed -
589 infected - recovered - deceased (SEIRD) model with heterogeneous diffusion. *Applied Mathematics Letters*. 2020; 111: 106617.
590 <https://doi.org/10.1016/j.aml.2020.106617>.
- 591 [15] Cooke KL, Driessche PVD. Analysis of an SEIRS epidemic model with two delays. *Journal of Mathematical Biology*. 1996; 35(2):
592 240-260. <https://doi.org/10.1007/s002850050051>.

- 593 [16] Okuonghae D, Oname A. Analysis of a mathematical model COVID-19 population dynamics in Lagos, Nigeria. *Chaos, Solitons*
594 & *Fractals*. 2020; 139: 110032. <https://doi.org/10.1016/j.chaos.2020.110032>.
- 595 [17] Davies NG, Klepac P, Liu Y, et al. Age-dependent effects in the spread and control of COVID-19 epidemics. *Nature Medicine*.
596 2020; 26: 1205-1211. <https://doi.org/10.1038/s41591-020-0962-9>.
- 597 [18] Davies NG, Kucharski AJ, Eggo RM, et al. Effects of non-pharmaceutical interventions on COVID-19 cases, deaths, and demand for
598 hospital services in the UK: a modelling study. *The Lancet*. 2020; 7(5): e375-e385. [https://doi.org/10.1016/S2468-2667\(20\)30133-X](https://doi.org/10.1016/S2468-2667(20)30133-X).
- 599 [19] Kassa SM, Njagarah JBH., Terefe YA. Analysis of the mitigation strategies for COVID-19: From mathematical modelling
600 perspective. *Chaos, Solitons & Fractals*. 2020; 138: 109968. <https://doi.org/10.1016/j.chaos.2020.109968>.
- 601 [20] Stadnytskyi V, Bax CE, Bax A, et al. The airborne lifetime of small speech droplets and their potential importance in SARS-CoV-2
602 spread. *PNAS*. 2020; 117(22): 11875-11877. <https://doi.org/10.1073/pnas.2006874117>.
- 603 [21] Ribeiro MHDM, Silva RGD, Mariani VC, et al. Short-term forecasting COVID-19 cumulative confirmed cases: Perspectives for
604 Brazil. *Chaos, Solitons & Fractals*. 2020; 135:109853. <https://doi.org/10.1016/j.chaos.2020.109853>.
- 605 [22] Chakraborty T, Ghosh I. Real-time forecasts and risk assessment of novel coronavirus (COVID-19) cases: A data-driven analysis.
606 *Chaos, Solitons & Fractals*, 2020, 135: 109850. <https://doi.org/10.1016/j.chaos.2020.109850>.
- 607 [23] Li SJ, Song K, Yang BR, et al. Preliminary assessment of the COVID-19 outbreak using 3-staged model e-ISHR. *Journal Shanghai*
608 *Jiaotong University (Science)*. 2020; 25(2): 157-164. <https://doi.org/10.1007/s12204-020-2169-0>.
- 609 [24] Zhang LY, Li DC, Ren JL. Analysis of COVID-19 by Discrete Multi-stage Dynamics System with Time Delay. *Geomatics and*
610 *Information Science of Wuhan University*. 2020; 45(5): 658-666. <https://doi.org/10.13203/j.whugis20200206>.
- 611 [25] Lymperopoulos IN. #stayhome to contain contain COVID-19: Neuro-SIR-Neuro dynamical epidemic modeling of infection
612 patterns in social networks. *Expert Systems with Applications* 165,113970. <https://doi.org/10.1016/j.eswa.2020.113970>.
- 613 [26] Bouchnita, A., Jebrane, A., 2020. A hybrid multi-scale model of COVID-19 spread dynamics to assess the potential of
614 non-pharmaceutical interventions. *Chaos, Solitons & Fractals*. 2020; 138: 109941. <https://doi.org/10.1016/j.chaos.2020.109941>.
- 615 [27] Lin QY, Zhao S, Gao DZ, et al. A conceptual model for the coronavirus disease 2019 (COVID-19) outbreak in Wuhan,
616 China with individual reaction and governmental action. *International Journal of Infectious Diseases*. 2020; 93: 211-216.
617 <https://doi.org/10.1016/j.ijid.2020.02.058>.
- 618 [28] Fang YQ, Nie YT, Penny M. Spread dynamics of the COVID-19 outbreak and effectiveness of government interventions: A
619 data-driven analysis. *Journal of Medical Virology*. 2020; 92(6): 645-659. <https://doi.org/10.1002/jmv.25750>.
- 620 [29] Tang B, Wang X, Li Q, et al. Estimation of the spread risk of the 2019-nCoV and its impact for public health interventions.
621 *Journal of Clinical Medicine*. 2020; 9(2): 462. <https://doi.org/10.3390/jcm9020462>.
- 622 [30] Chu DK, Duda S, Solo K, et al. Physical distancing, Face masks, and eye protection to prevent person-to-person spread of
623 SARS-CoV-2 and COVID-19: A systematic review and meta-analysis. *Lancet*. 2020; 72(4): 1500.
624 <https://doi.org/10.1016/j.jvs.2020.07.040>.
- 625 [31] Ma ZH, Wang SF, Li XH. A generalized infectious model induced by the contacting distance (CTD). *Nonlinear Analysis: Real*
626 *World Applications*. 2020; 54: 103113. <https://doi.org/10.1016/j.nonrwa.2020.103113>.

- 627 [32] Gostic K, Gomez ACR, Mummah RO, et al. Estimated effectiveness of symptom and risk screening to prevent the spread of
628 COVID-19. *eLife* 2020; 9: e55570. <https://doi.org/10.7554/eLife.55570>.
- 629 [33] Wells C.R. Sah, P, Moghadas SM, et al. Impact of international travel and border control measures on the global spread of the
630 novel 2019 coronavirus outbreak. *PANS*. 2020; 117(13): 7504-7509. <https://doi.org/10.1073/pnas.2002616117>.
- 631 [34] Hellewell JH, Abbott S, Gimma A, et al. Feasibility of controlling COVID-19 outbreaks by isolation of cases and contacts. *Global
632 Health*. 2020; 4(8): e488-e496. [https://doi.org/10.1016/S2214-109X\(20\)30074-7](https://doi.org/10.1016/S2214-109X(20)30074-7).
- 633 [35] Wölfel R, Corman VM, Guggemos W, et al. Virological assessment of hospitalized patients with COVID-2019. *Nature*. 2020; 281:
634 465-469. <https://doi.org/10.1038/s41586-020-2196-x>.
- 635 [36] Rosa GL, Bonadonna L, Lucentini Luca, et al. Coronavirus in water environments: Occurrence, persistence and concentration
636 methods - A scoping review. *Water Research*, 2020; 179: 115899. <https://doi.org/10.1016/j.watres.2020.115899>.
- 637 [37] Leclerc QJ, Fuller NM, Knight LE. et al. What settings have been linked to SARS-CoV-2 spread cluster? [version 1; peer review:1
638 approved with reservations]. *Wellcome Open Research*, 2020; 5: 83. <https://doi.org/10.12688/wellcomeopenres.15889.1>.
- 639 [38] Lu JY, Gu, Li JN, Xu KB, CH, et al. COVID-19 outbreak associated with Air conditioning in restaurant, Guangzhou, China, 2020.
640 *Emerging Infectious Diseases*. 2020; 26(7): 1682-1631. <https://dx.doi.org/10.3201/eid2607.200764>.
- 641 [39] Morawska L, Cao JJ. Airborne spread of SARS-CoV-2: The world should face the reality. *Environment International*. 2020; 139:
642 105730. <https://doi.org/10.1016/j.envint.2020.105730>.
- 643 [40] Dehning J, Zierenberg J, Spitzner FP, et al. Inferring change point in the spread of COVID-19 reveals the effectiveness of
644 interventions. *Science*. 2020; 6500(369): eabb9789. <https://doi.org/10.1126/science.abb9789>.
- 645 [41] Thu TPB, Ngoc PNH, Hai NM, et al. Effect of the social distancing measures on the spread of COVID-19 in 10 highly infected
646 countries. *Science of the Total Environment*. 2020; 742: 140430. <https://doi.org/10.1016/j.scitotenv.2020.140430>.
- 647 [42] Barmparis GD, Tsironis GP. Estimating the infection horizon of COVID-19 in eight counties with a data-driven approach. *Chaos,
648 Solitons & Fractals*. 2020; 135: 109842. <https://doi.org/10.1016/j.chaos.2020.109842>.
- 649 [43] Han WG. Data-driven and model-driven spatiotemporal data mining-respective case study in traffic flow data and epidemic data,
650 Chinese Academy of Sciences. 2006. <http://ir.igsnr.ac.cn/handle/311030/106>
- 651 [44] Franch-Pardo I, Napoletano BM, Rosete-Verges F, et al. Spatial analysis and GIS in the study of COVID-19. A review. *Science of
652 the Total Environment*. 2020; 739: 140033. <https://doi.org/10.1016/j.scitotenv.2020.140033>.
- 653 [45] Feng MX, Fang ZX, Lu XB, et al. Traffic Analysis Zone-Based Epidemic Estimation Approach of COVID-19 Based on Mobile
654 Phone Data: An Example of Wuhan. *Geomatics and Information Science of Wuhan University*. 2020, 45(5): 651-657, 681.
655 <https://doi.org/10.13203/j.whugis20200141>.
- 656 [46] Sugg MM, Spaulding RJ, Lane SJ, et al. Mapping community-level determinants of COVID-19 spread in nursing homes: A
657 multi-scale approach. *Science of the Total Environment*. 2020, 752: 141946. <https://doi.org/10.1016/j.scitotenv.2020.141946>.
- 658 [47] Ren HY, Zhao L, Zhang A, et al. Early forecasting of the potential risk zones of COVID-19 in China's megacities. *Science of the
659 Total Environment*. 2020; 729: 138995. <https://doi.org/10.1016/j.scitotenv.2020.138995>.
- 660 [48] Fang ZX. Thinking and challenges of crowd dynamics observation from the perspectives of public health and public security.

661 Geomatics and Information Science of Wuhan University. 2020; 45(12): 1847-1856. <https://doi.org/10.13203/j.whugis20200422>.

662 [49] Cao ZD. Mathematical modeling and spatial analysis of spatiotemporal data-case study based on SARS epidemic in Guangzhou.
663 Chinese Academy of Sciences. 2008. <http://ir.igsnr.ac.cn/handle/311030/1774>.

664 [50] Dong E, Du H, Gardner L. An interactive web-based dashboard to track COVID-19 in real time. *Lancet Infectious*
665 *Diseases*. 2020; 20(5): 422-534. [https://doi.org/10.1016/S1473-3099\(20\)30120-1](https://doi.org/10.1016/S1473-3099(20)30120-1).

666 [51] Cui HJ, Hu T. Nonlinear regression in COVID-19 forecasting (in Chinese). *SCIENTIA SINICA Mathematica*. 2020;
667 (50): 1-12. <https://engine.scichina.com/doi/10.1360/SSM-2020-0055>.

668 [52] Xia JZ, Zhou Y, Li Z, et al. COVID-19 risk assessment driven by urban spatiotemporal big data: case study of
669 Guangdong-Hong Kong-Macao Greater Bay Area. *Acta Geodaetica et Cartographica Sinica*. 2020; 49(6): 671-680.
670 <http://xb.sinomaps.com/CN/10.11947/j.AGCS.2020.20200080>.

671 [53] Alberti T, Faranda D. On the uncertainty of real-time predictions of epidemic growths: A COVID-19 case study for
672 China and Italy. *Communications in Nonlinear Science and Numerical Simulation*. 2020; 90: 105372.
673 <https://doi.org/10.1016/j.cnsns.2020.105372>.

674 [54] Guo L, Yang WQ, Bi YF. Research on the Scale of Daily Life Unit Based on Residents' Travel Characteristics. *China*
675 *Academic Journal Electronic Publishing House*. 2016; 1004-1015.
676 <https://kns.cnki.net/KCMS/detail/detail.aspx?dbcode=CPFD&filename=CSJT201604001098>.

677 [55] Cauchemez S, Fraser C, Wan MD, et al. Middle east respiratory syndrome coronavirus: quantification of the extent of
678 the epidemic, surveillance biases, and transmissibility. *The Lancet Infectious Diseases*. 2020; 1(14): 50-56.
679 [https://doi.org/10.1016/S1473-3099\(13\)70304-9](https://doi.org/10.1016/S1473-3099(13)70304-9).

680 [56] Viguerie A, Lorenzo G, Auricchio F, et al. Simulating the spread of COVID-19 via a spatially-resolved susceptible -
681 exposed - infected - recovered - deceased (SEIRD) model with heterogeneous diffusion. *Applied Mathematics Letters*,
682 2020; 111: 106617. <https://doi.org/10.1016/j.aml.2020.106617>.

Figures

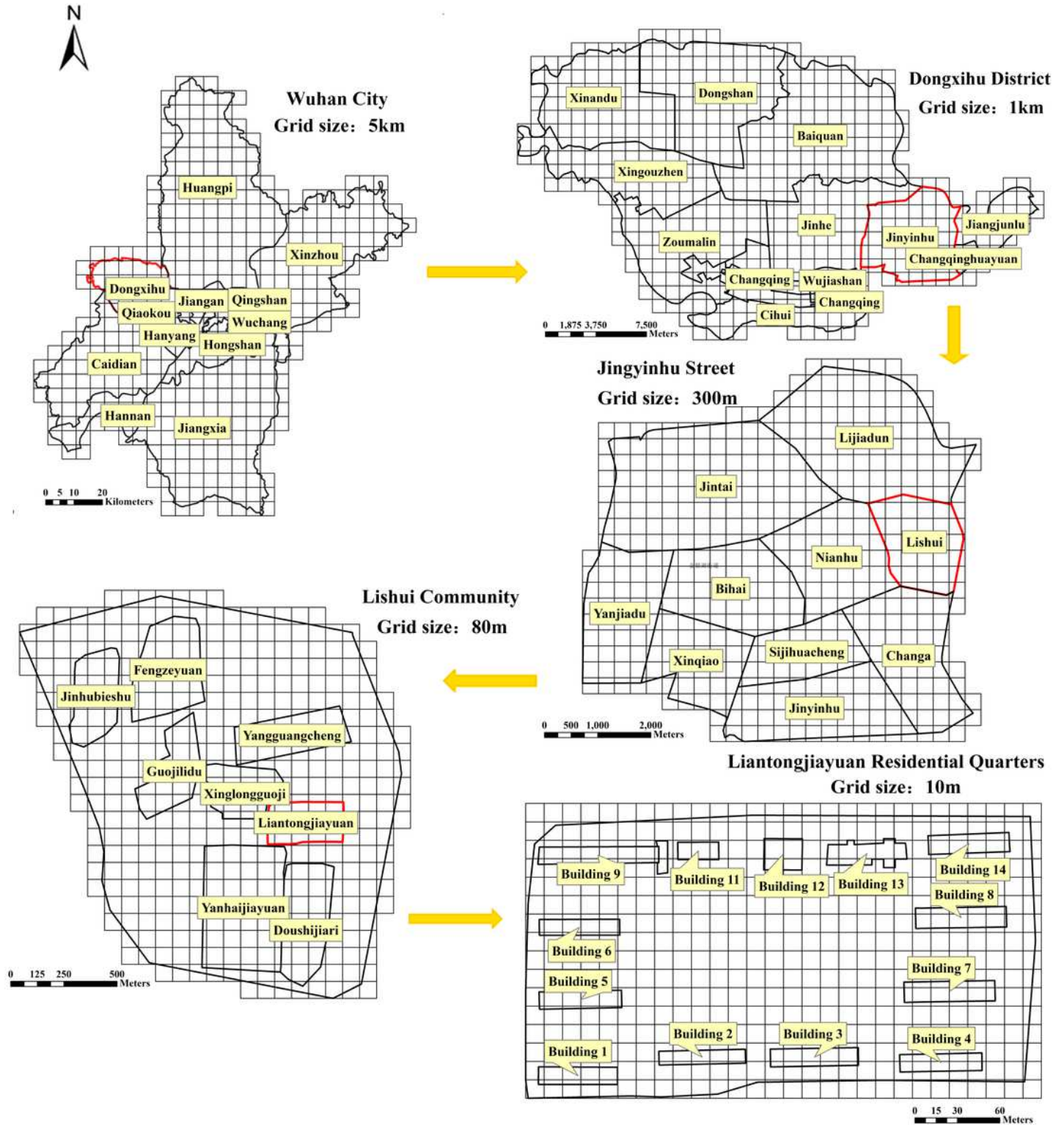


Figure 1

Grid filling diagram of traditional prevention and control unit. Note: The designations employed and the presentation of the material on this map do not imply the expression of any opinion whatsoever on the part of Research Square concerning the legal status of any country, territory, city or area or of its

authorities, or concerning the delimitation of its frontiers or boundaries. This map has been provided by the authors.

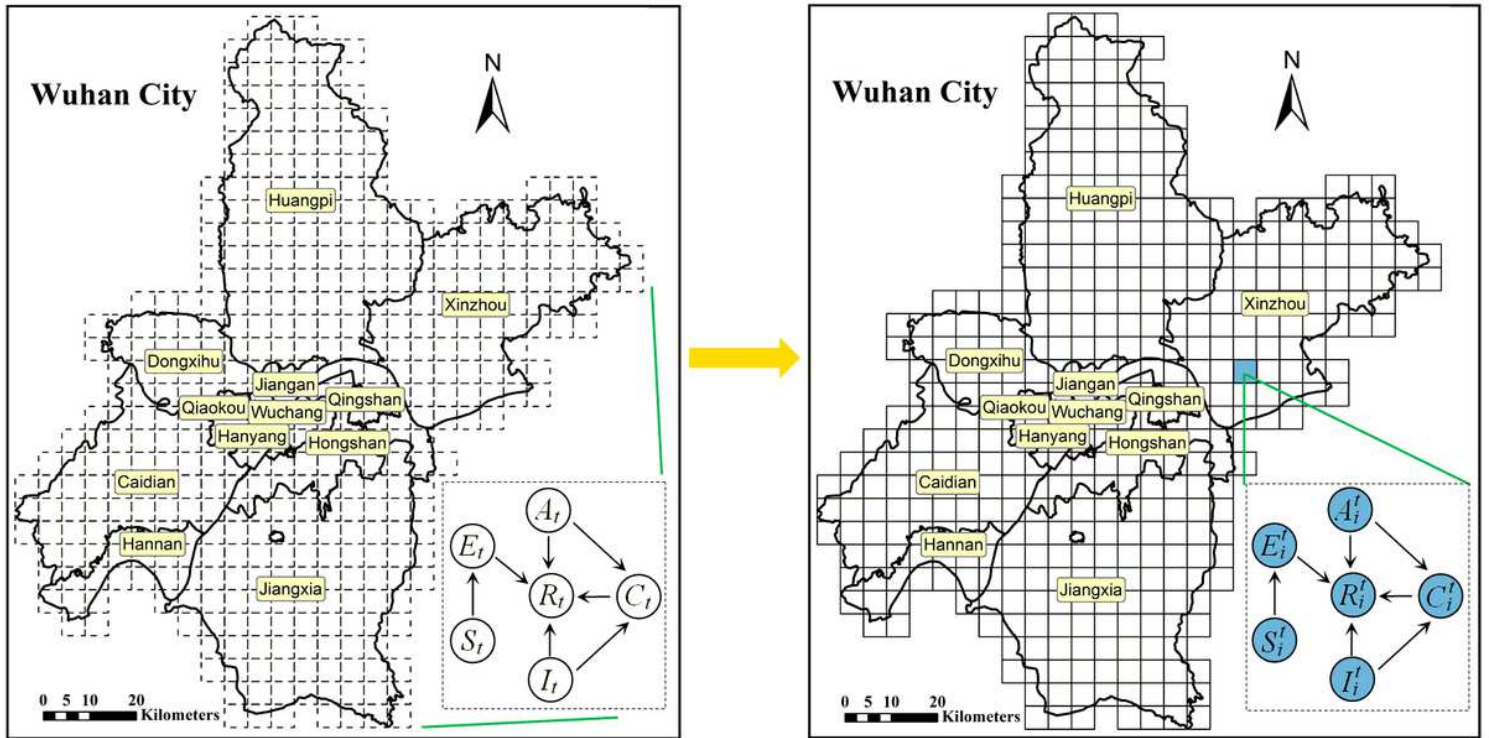


Figure 2

Schematic diagram of the quarantine measure model based on a discrete grid. Note: The designations employed and the presentation of the material on this map do not imply the expression of any opinion whatsoever on the part of Research Square concerning the legal status of any country, territory, city or area or of its authorities, or concerning the delimitation of its frontiers or boundaries. This map has been provided by the authors.

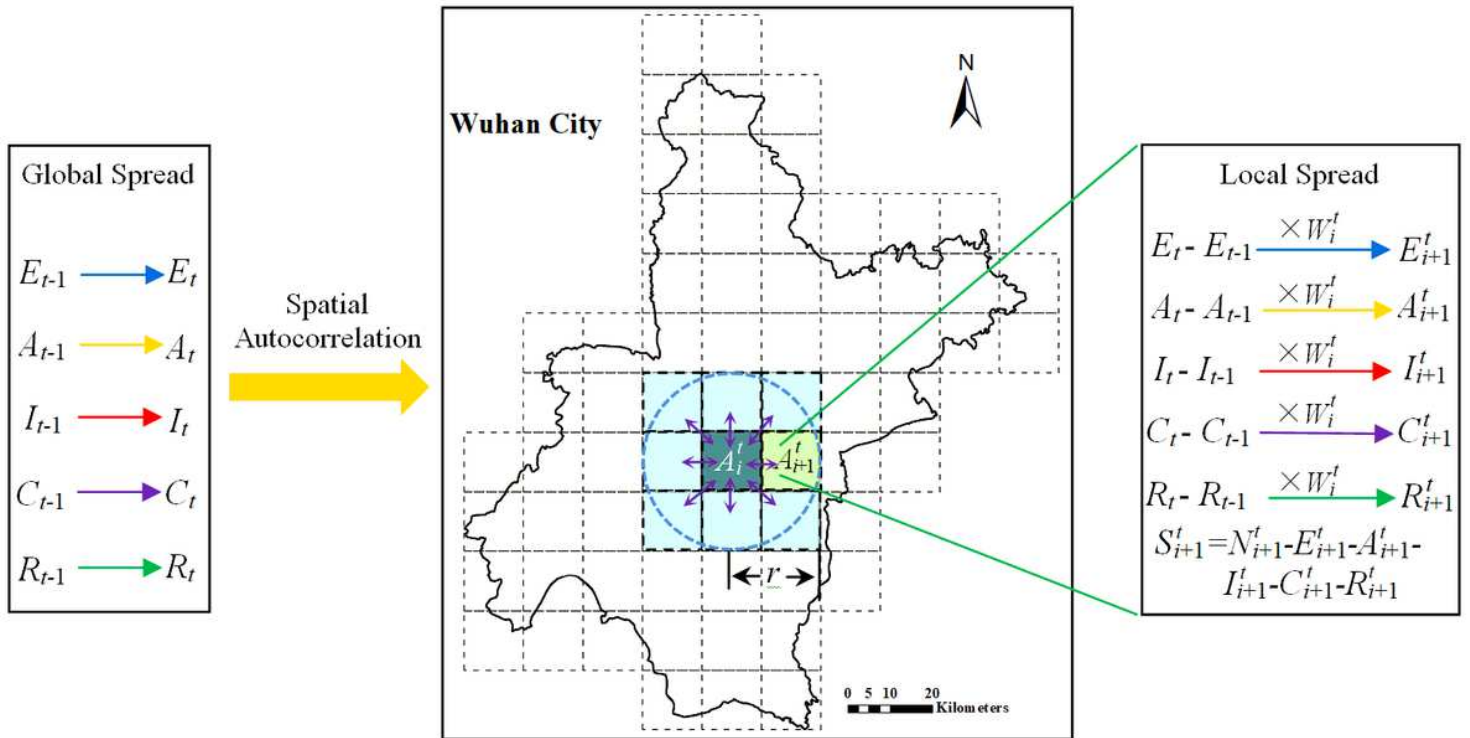


Figure 3

Spatiotemporal spread model for infectious diseases based on a discrete grid. Note: The designations employed and the presentation of the material on this map do not imply the expression of any opinion whatsoever on the part of Research Square concerning the legal status of any country, territory, city or area or of its authorities, or concerning the delimitation of its frontiers or boundaries. This map has been provided by the authors.

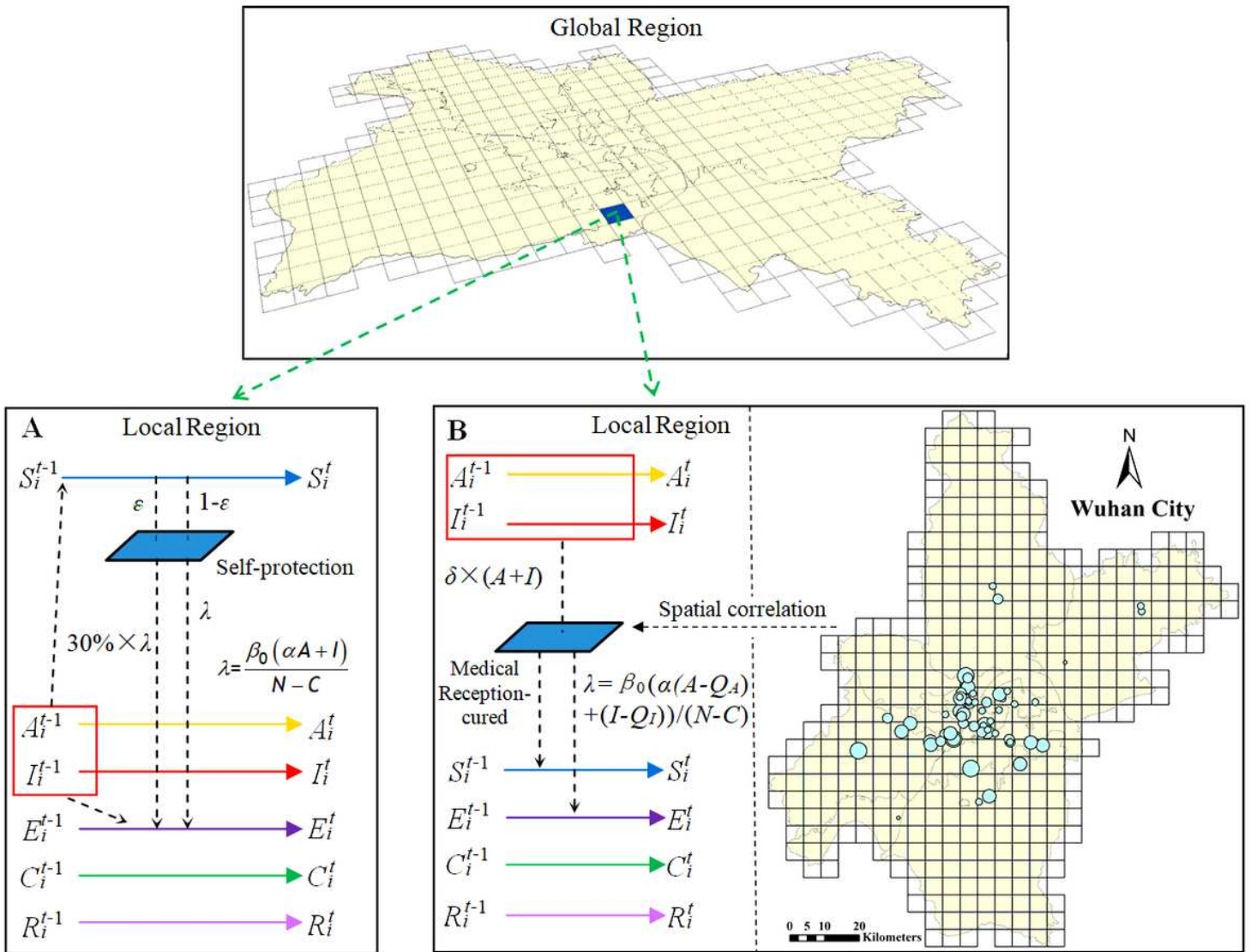
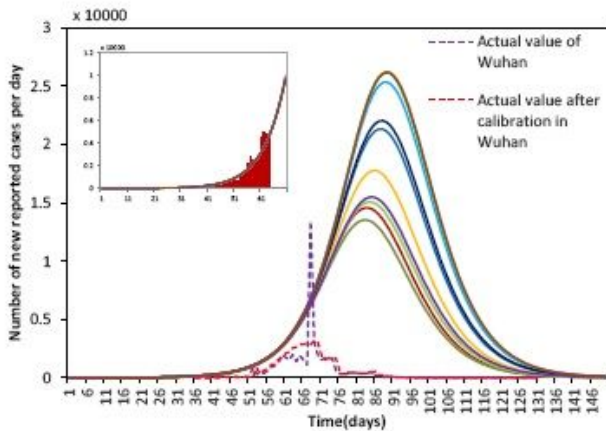
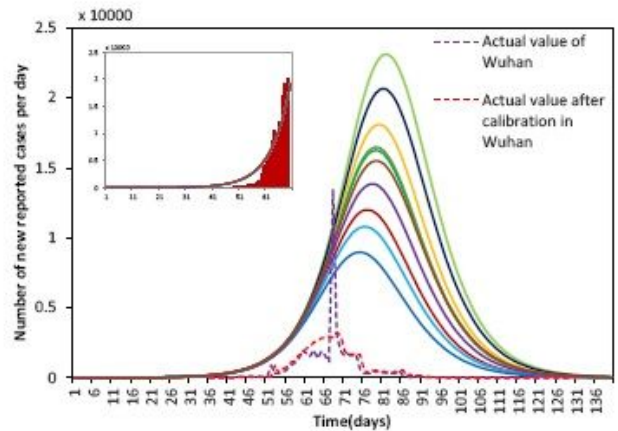


Figure 4

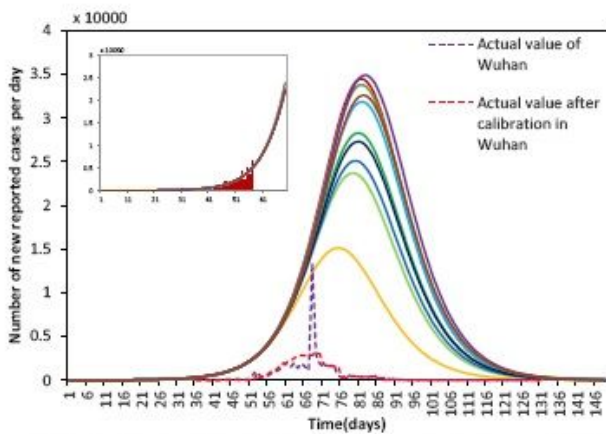
Schematic diagram of medical reception-cured measure (A) and self-protection measure (B). Note: The designations employed and the presentation of the material on this map do not imply the expression of any opinion whatsoever on the part of Research Square concerning the legal status of any country, territory, city or area or of its authorities, or concerning the delimitation of its frontiers or boundaries. This map has been provided by the authors.



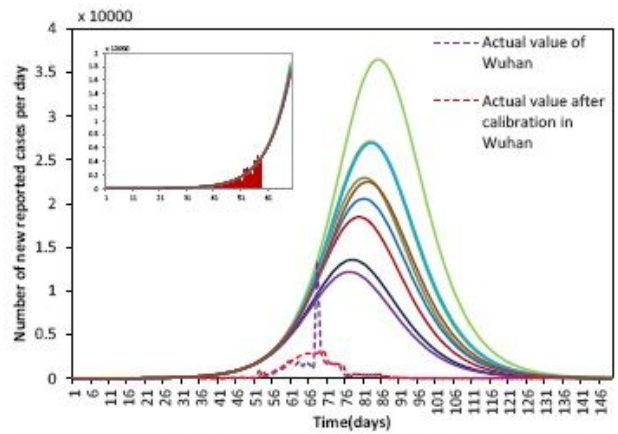
(a) Early UK data to simulate the original spread of COVID-19



(b) Early US data to simulate the original spread of COVID-19



(c) Early Spain data to simulate the original spread of COVID-19



(d) Early German data to simulate the original spread of COVID-19

Figure 5

The number of newly reported cases per day of original state simulated by genetic algorithm (Small chart section: the red histogram represents the early epidemic data of each country, and the curve is the original spread state curve of COVID-19 in each country. Here, the starting time of X coordinate in the UK, the US, Spain, and Germany is January 31, 2020, January 20, 2020, February 1, 2020, and January 27, 2020, respectively; big graph section: the solid-line curve is the original spread state curve of Wuhan. The red dotted-line curve shows the actual number of newly reported cases in Wuhan after calibration, and the purple dotted-line curve represents the actual number of newly reported cases in Wuhan. Here, the starting time of X coordinate in the Wuhan is December 28, 2020 [9])

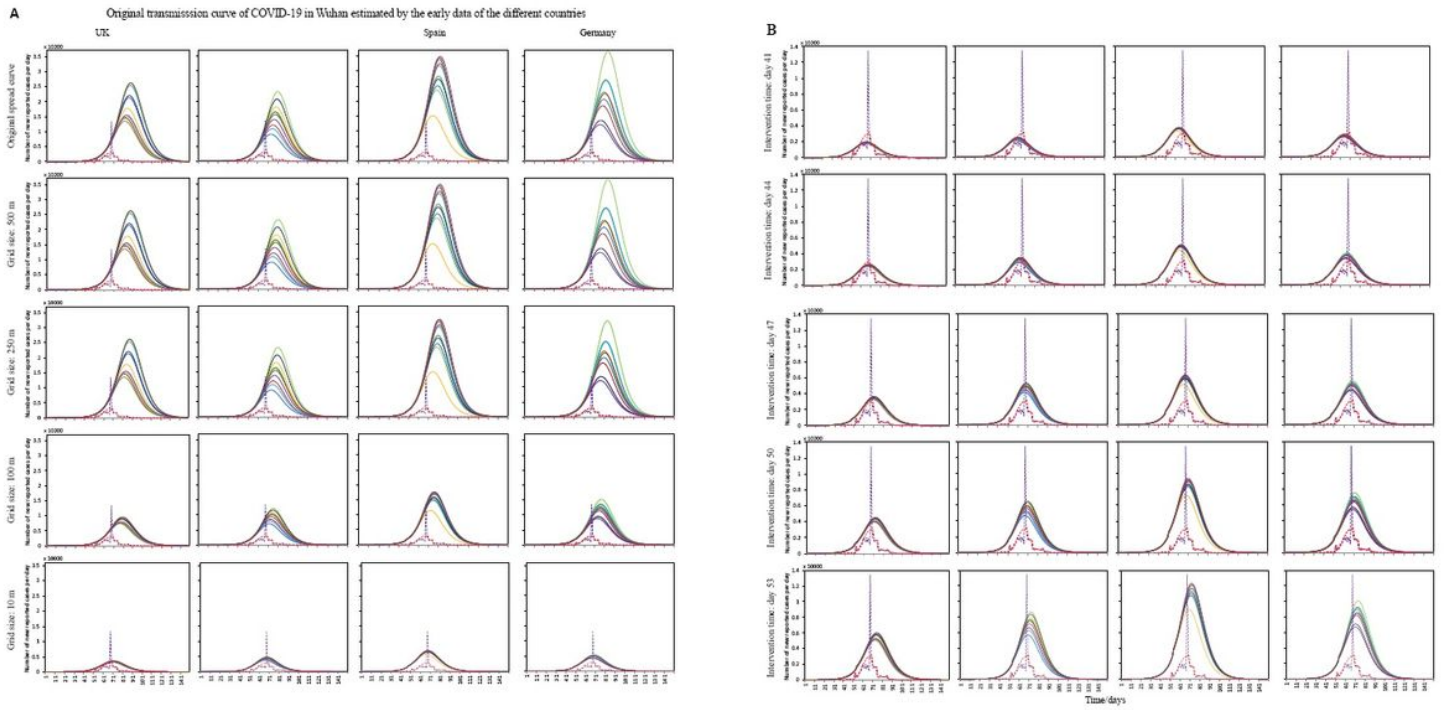


Figure 6

The change curve of newly reported cases per day in Wuhan under different quarantine measure

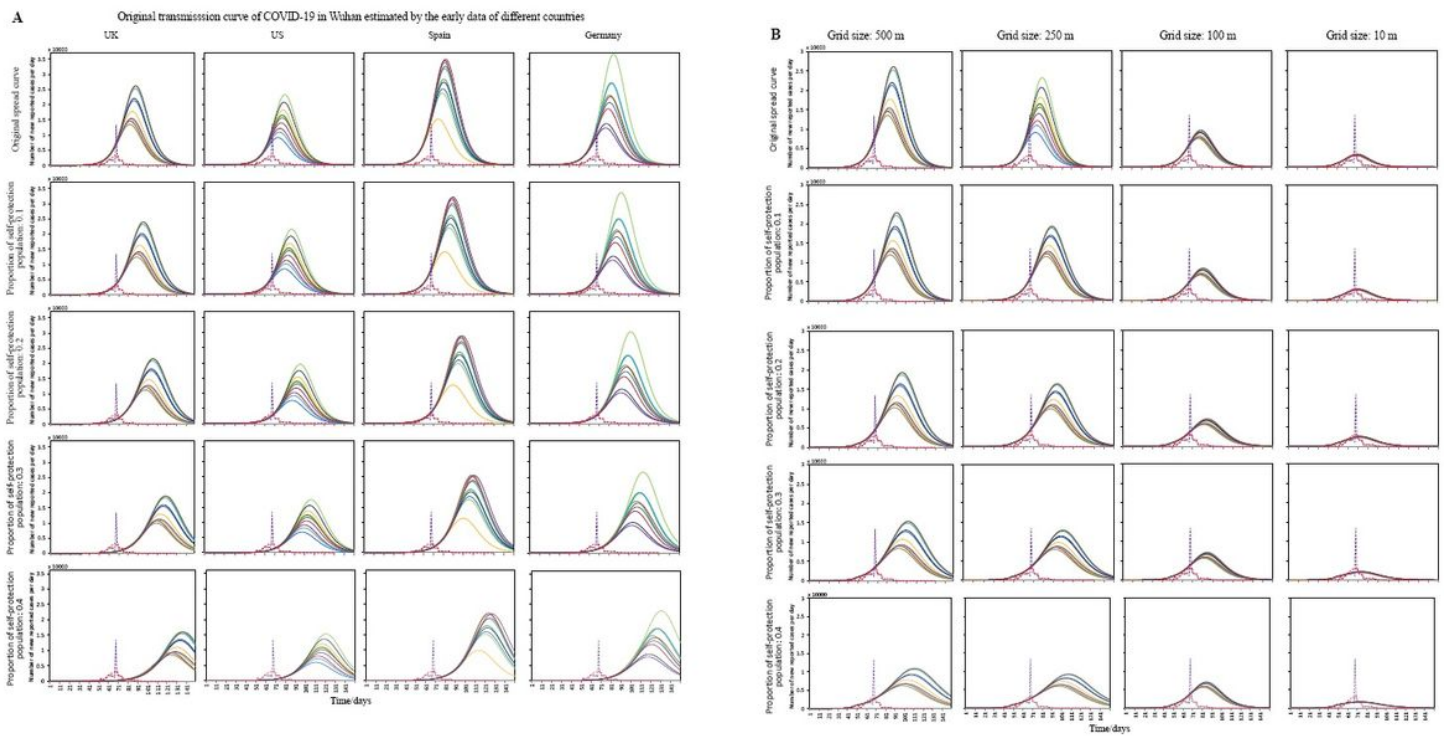


Figure 7

The change curve of newly reported cases per day in Wuhan under different self-protection measure

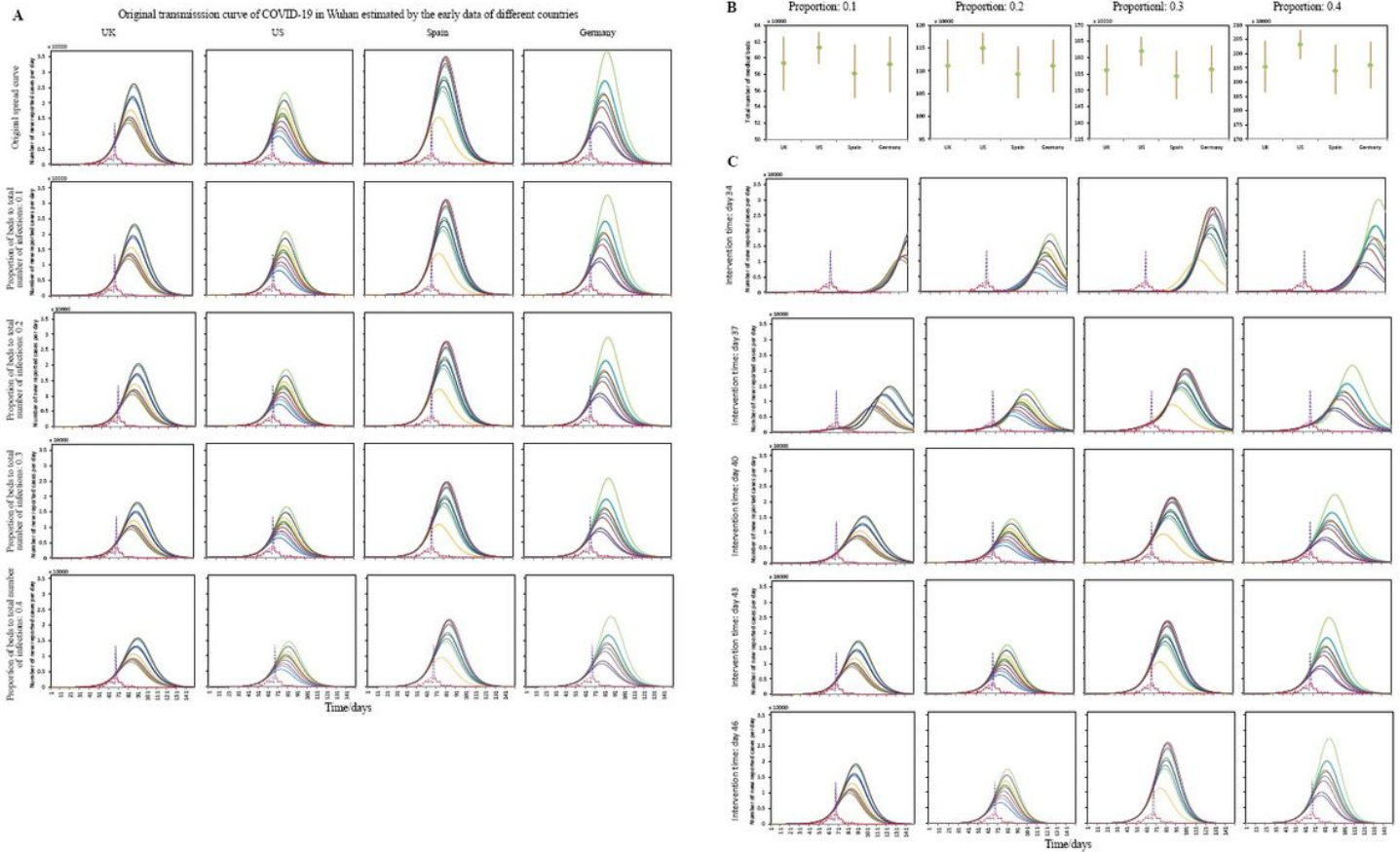


Figure 8

The change curve of newly reported cases per day in Wuhan under the different medical reception-cured measure (the length of the yellow vertical line and the green prism points indicates the 95% confidence interval and the median values of the total number of invested beds corresponding to 10 curves in group B, respectively)

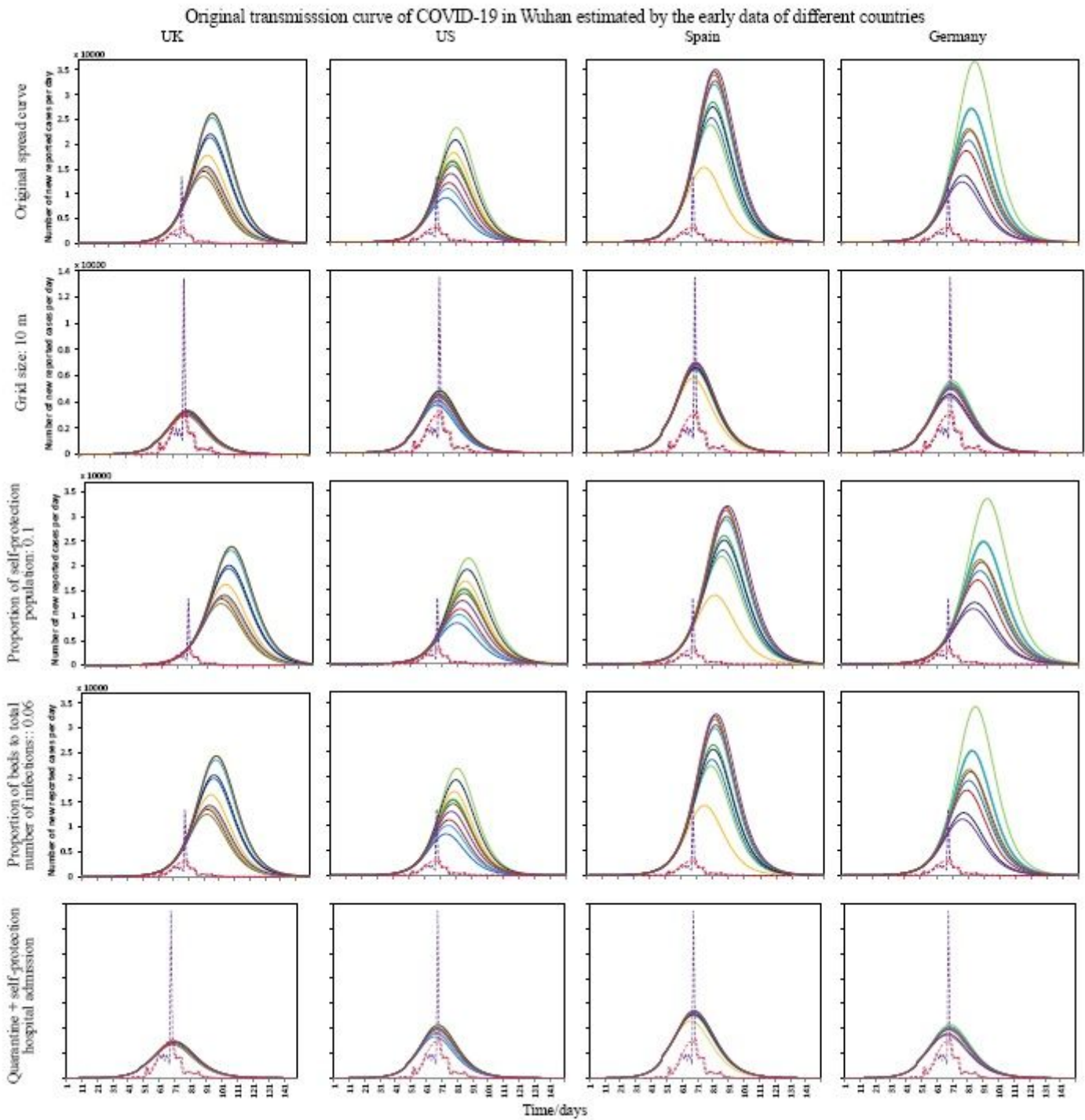


Figure 9

The change curve of newly reported cases per day in Wuhan under actual interventions

Supplementary Files

This is a list of supplementary files associated with this preprint. Click to download.

- [Table.doc](#)